Journal of Investigations on Engineering & Technology
Volume 2, Issue 2, 26.12, 2019
ISSN: 2687-3052

Effect of Rb Substitution on the Structural, Physical and Superconducting Properties of Bi-2212 Superconductor

İbrahim ERGİN*[1], Bekir ÖZÇELİK[1], Andres SOTELO[2], M.A. MADRE[2]

[1]Çukurova Üniversitesi, Fen-Edebiyat Fakültesi, Fizik Bölümü, 01330, Adana, Türkiye
[2] *ICMA (CSIC-Universidad de Zaragoza). María de Luna*, 50018, Zaragoza, İspanya

(Received: 24.10.2019, Accepted: 25.12.2019, Published Online: 26.12.2019)

Keywords
Bi-2212
Rubidium substitution
Magnetic Properties

Abstract: In this research, the effects of Rubidium (Rb) inclusion on the microstructural, physical and superconducting properties of $Bi_2Sr_2Ca_{1-x}Rb_xCu_2O_{8+y}$ with x=0.0, 0.025, 0.05, 0.075, 0.10, and 0.125, superconductor have, in detail, been studied. For this purpose, the samples were prepared through the classical solid state reaction route. From the XRD patterns, the crystal symmetries of samples were determined as pseudo tetragonal and consist of dominant Bi-2212 phase together with small amount of secondary phases. SEM-EDX results have confirmed that the major phase is related to Bi-2212, with minor amounts of secondary phases. In magnetization versus temperature measurements, very sharp diamagnetic transition is observed. The superconducting critical temperatures, T_C, for all samples are obtained around 80 K. From *M-H* measurement, it has been found that all samples have very narrow loop areas. By using the data from *M-H* measurements in the Bean model, the intragranular critical field, J_C, has been determined. It has been found that the pure Bi-2212 (x=0.0) sample shows the highest superconducting properties and the largest J_C values ($2{,}2x10^4$ A/cm^2 at 10 K).

1. Introduction

Bi-based superconductors with Bi-Sr-Ca-Cu-O (BSCCO) content and stoichiometric 2-2-1-2 respectively are called Bi-2212, which are into the high-temperature superconductor structure. It is too easy to produce in terms of their oxidized structure and contain no rare earth elements and is not easily affected by oxygenated environments. Moreover, it has high current carrying capacity, high magnetic field carrying capacity and the high transition temperature to superconductivity makes this type of superconductor more attractive in industry. However, mechanical properties such as weak bonds, brittleness and weak elasticity in the structure of this superconductor family restrict their application. The BSCCO superconductor family with a chemical structure has n = 1, 2 and 3 phase structures (Bi-2201, Bi-2212 and Bi-2223 respectively) depending on CuO_2 content [1-3].

It has been stated the superconducting properties of the BSCCO system can be improved by alkaline metals substitutions, since their +1 valence state generates a variation in the charge carrier concentration. In addition, their ionic radii, ranging in between 73–181 pm, superpose with the Bi, Sr, Ca, and Cu ones [4-6]. In this work, the optimum amount of Rb substitution into BSCCO system by replacing Ca will be determined through the variation of structural, physical and magnetic properties of the doped systems as a function of Rb-concentration.

2. Experimental Details

$Bi_2Sr_2Ca_{1-x}Rb_xCu_2O_y$ samples were produced by solid state method at x = 0.0, 0.025, 0.05, 0.075, 0.1, and 0.125 combinations. Oxidized and carbonate powders used are Bi_2O_3, $SrCO_3$, $CaCO_3$, Rb_2O and CuO. Oxidized and carbonate powders were mixed separately for each sample. The mixtures were well mixed by milling in an agate mortar and calcined twice at 750 and 800°C for 12 h in order to decompose the alkaline-earth carbonates. The purpose of the calcination course is to ensure the decomposition of carbonated structures. The carbonated structures are

*İlgili yazar: erginibrahim2@gmail.com ORCID: 0000-0002-6778-5442

separated during the sintering process after calcination and can form bubble structures. In this case it may have a slowing or stopping effect on the formation of the desired crystal structure. Rigaku Minifilex, XRD device, which emits CuKa radiation at a certain ratio of 10 to 70 degrees (2θ) at room temperature as powder, was used to determine the phases in the heat treated material. From these phases, crystal lattice parameters were calculated with an uncertainty of ± 0.001. For surface morphology and elemental analysis, LEO Evo-40 VPX scanning electron microscopy (SEM) and energy dispersive spectroscopy (EDS) were used. For magnetic measurements, the 7304 model Vibrating Sample Magnetometer of Lake Shore was used to determine the transition temperature to superconductivity and to observe the magnetization change in the ±1 Tesla magnetic field.

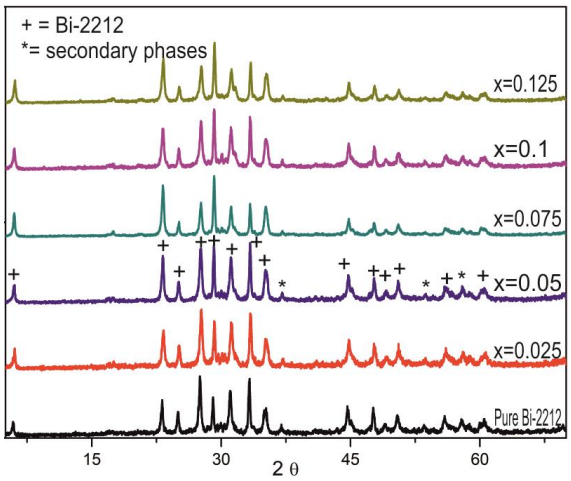

Fig. 1. XRD patterns for all samples with increasing Rb concentration from bottom to top

3. Result and Discussion

As can be observed from XRD patterns given in Fig.1, the main phase labeled as (+) is Bi-2212 one together with minor phases (*), for all different Rb-substitution. As can be seen from the XRD results, Rb entered Bi-2212 phase due to none existence of Rb content peaks. The crystal symmetry is found as pseudo tetragonal with the lattice parameters, calculated by using the least squares method, are a=b=5.398 Å and c=30.685 Å, in all cases.

Fig. 2 shows the phases according to the specific contrast setting on the material surface. The identities of the phases are determined according to the elemental analysis (EDX) at the places marked with 1, 2 and 3. EDS analysis of these contrasts has allowed to associate each of them to different phases: major gray contrast (indicated by #1) in all micrographs corresponds to the Bi-2212 superconducting phase, while white (#2) and dark gray (#3) have been associated to $Bi_{2+x}(Sr,Ca)_2O_{6+d}$ (without Cu phase), and $(Sr,Ca)CuO_2$ (without Bi phase) secondary phases, respectively.

Magnetization, M, versus temperature is exhibited in Fig. 3, for all samples. All data were generated in a cooled mode under magnetic field from 20 K to 100 K under 100 Oe magnetic field. By increasing the sensitivity in a temperature range close to the transition temperature, T_C, it is provided to determine the transition temperatures to an exact value. From the M-T graph, the critical transition temperatures for all samples were deduced in a very similar way. It can be seen from Table 1 that all samples, regardless of the concentration of the Rb additive, have a critical transition temperature of around 80 K.

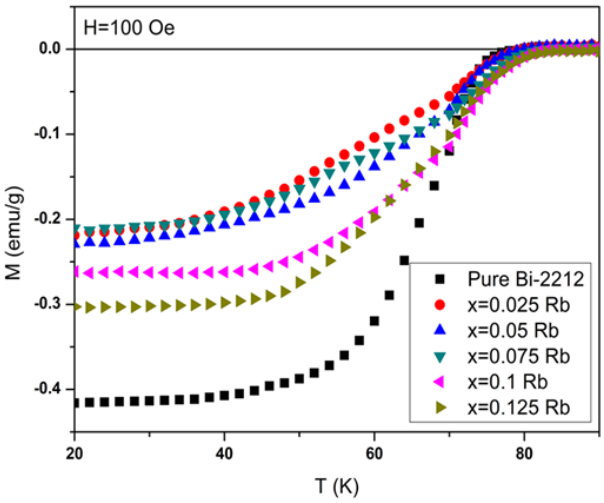

Fig. 3. Magnetization (M) versus temperature (T), for all samples.

It is likely that diamagnetic behavior makes it difficult to infiltrate the magnetic field between these grain boundaries due to the strong connection between the grain boundaries.

The M–H loops measured at 10 K, between ±1 Tesla applied external fields, and determined under ZFC mode, are presented in Fig. 4. All samples exhibit very narrow hysteresis and the area of these hysteresis loops decrease depending on concentration. M-H data were used in Eq. 1, proposed for quadrangular samples, in the well-known critical Bean model [7]

$$J_C = 20\frac{\Delta M}{a(1-\frac{a}{3b})} \qquad (1)$$

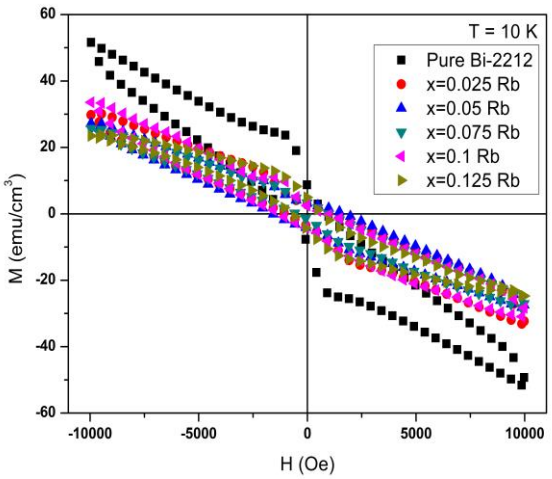

Fig. 4. Magnetization, *M*, versus magnetic field, *H*, for all samples

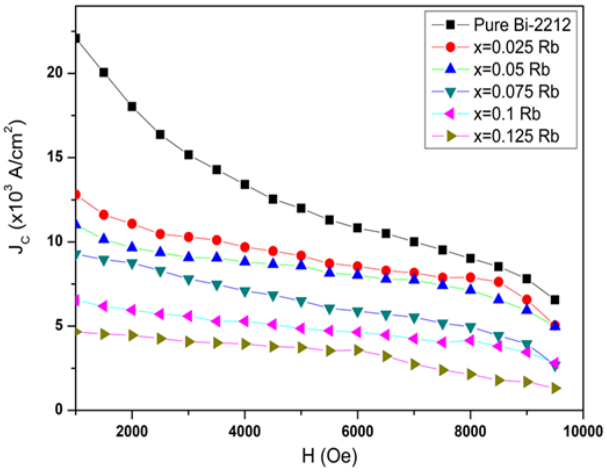

Fig.5. Critical current density, J_C, versus magnetic field, *H*, for all samples.

Table 1. Critical transition temperature, T_C, for all samples

Samples	T_C (K)
x=0	80
x=0.025	78.6
x=0.05	80.3
x=0.075	79.5
x=0.1	79
x=0.125	82

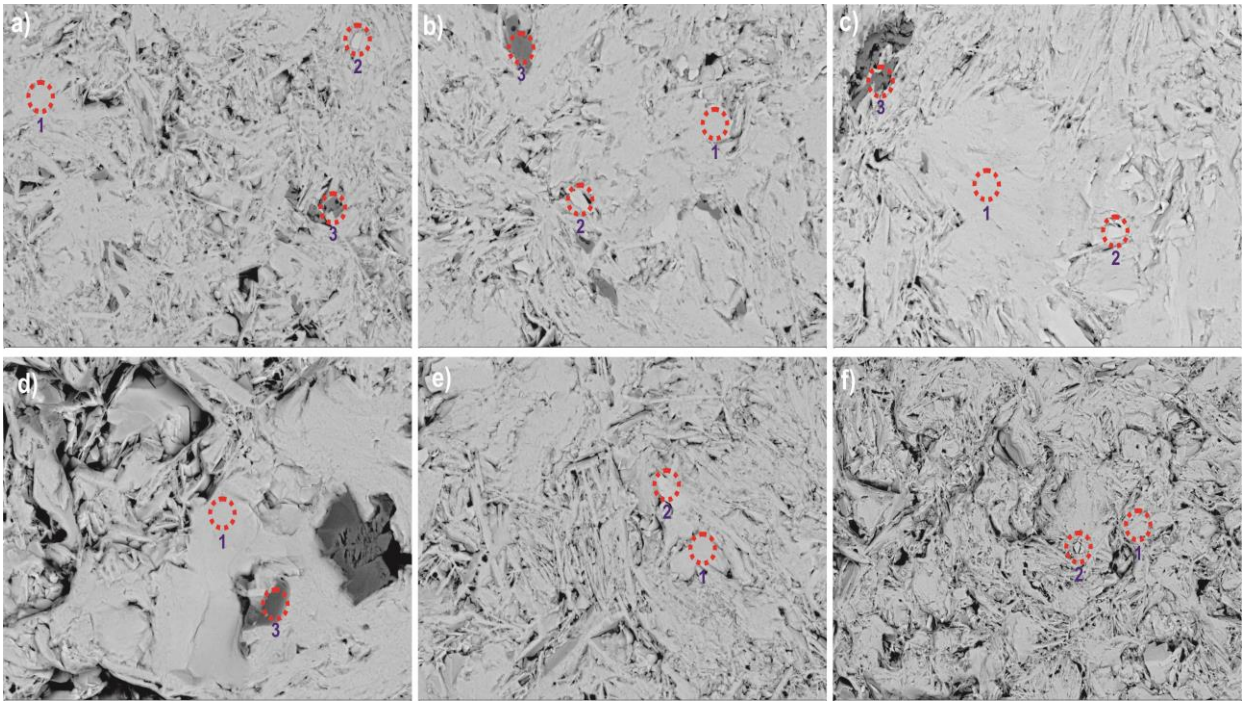

Fig. 2. SEM micrographs for all samples. (a) x=0.0, (b) x=0.025, (c) x=0.05, (d) x=0.075, (e) x=0.1, (f) x=0.125

where $\Delta M = M_+ - M_-$ is measured in electromagnetic units per 200 Oe, *a* and *b* are the length of the sample plane perpendicular to the applied magnetic field. Using the Eq.1, the intragranular critical current density values, *Jc*, in ampéres per square centimeter are calculated for all samples, and the results obtained at 10 K are presented in Fig. 5. These data clearly show that the pure sample (x=0.0) possesses higher superconducting properties and has the largest J_C values ($2{,}2 \times 10^4$ A/cm^2 at 1000 Oe fields), which explicitly reduce when the magnetic field and the amount of Rb are raised. In this stage, it is possible to argue that the different type of secondary phases embedded in the crystal structure can reveal such a kind of results. According to the flux-pinning mechanism, those non-superconducting phases.

4. Conclusions

In summary, the structural, physical and magnetic properties of $Bi_2Sr_2Ca_{1-x}Rb_xCu_2O_{8+y}$ superconducting material with x=0.0, 0.025, 0.05, 0.075, 0.10, and 0.125 has been intensively studied. X-ray diffraction patterns indicate that all samples have main Bi-2212 phase. SEM micrographs and EDX results have shown that Bi-2212 was major phase with minor amounts of secondary phases. Diamagnetic transitions typical for granular materials were observed, when measuring magnetization versus temperature. The critical onset temperatures were around 80 K, independently of Rb content. *M-H* measurements have shown that the hysteresis loops are very narrow. The critical current field, J_C, of pure sample was found the highest value as $2{,}2 \times 10^4$ A/cm^2.

Acknowledgements

M. A. Madre, and A. Sotelo acknowledge the MINECO-FEDER (MAT2017-82183-C3-1-R), and Gobierno de Aragon-FEDER (Research Group T 54-17 R) for funding. The authors wish to acknowledge the use of Servicio General de Apoyo a la Investigación-SAI, Universidad de Zaragoza.

behave like very effective flux-pinning centers. Depending on the sizes of those secondary phases, the applied fields may diffuse into the sample, causing a decline in the critical current, *Jc*, values. The maximum *Jc* value obtained for the x=0.05 sample is almost near with the given in literature for Vanadium (2.53×10^5 A/cm^2) [8], and very similar to the obtained in Cs-substituted materials ($2{,}3 \times 10^4$ A/cm^2) [9]. This effect may be associated to the different cation sizes affecting the oxygen quantity and the number of charge carrier. In addition, comparison to Na-doped materials, a possible slight charge carrier concentration enhancement can be arisen by the lower effective attraction of the external electrons in the Rb^+ cations [10].

References

[1] H. Maeda, Y. Tanaka, M. Fukutumi, T. Asano, Jpn. J. Appl. Phys. 27, 209 (1988)

[2] C. Michel, M. Herviev, M.M. Borel, A. Grandin, F. Deslands, J. Provost, B. Raveav, Z. Phys. B 86, 421 (1987)

[3] J.M. Tarascon, W.R. McKinnon, P. Barboux, D.M. Hwang, B.G. Bagley, L.H. Greene, G.W. Hull, Y. LePage, N. Stoffel, and M. Giroud, Phys. Rev. B, 1988. 38(13): 8885-8892.

[4] B. Ozcelik, M. Gursul, A. Sotelo, M. A. Madre, J. Mater. Sci. Mater. Electron. 26, 441 (2015)

[5] B. Ozcelik, M. Gursul, A. Sotelo, M. A. Madre, J. Mater. Sci. Mater. Electron. **25**, 4476 (2014)

[6] L.D. Sykorova, O. Smrckova, V. Jakes, Phys. Stat. Sol. (C) **1**(7), 1952 (2004)

[7] C. P. Bean, Phys. Rev. Lett., 8, 250 (1962)

[8] Nane, O. & Özçelik, B. J Mater Sci: Mater Electron (2016)27:7633. https://doi.org/10.1007/s10854-016-4747-3

[9] I. Ergin, B. Özçelik, M.A. Madre, A.Sotelo, J Supercond.Nov.Magn. https://doi.org/10.1007/s10948-019-05150-4

[10] Özçelik, B., Gürsul, M., Sotelo, A. et al. J Mater Sci: Mater Electron (2015) 26: 441. https://doi.org/10.1007/s10854-014-2419-8